Oxygen transport and consumption in germinating seeds

Neil Budko (Delft University of Technology)
Alessandro Corbetta (Eindhoven University of Technology)
Bert van Duijn (Fytagoras) Sander Hille (Leiden University)*
Oleh Krehel (Eindhoven University of Technology)
Vivi Rottschäfer (Leiden University)
Linda Wiegman (Delft University of Technology)
Delyan Zhelyazov (Centrum voor Wiskunde en Informatica)

Abstract

Three mathematical models were formulated to describe the oxygen consumption of seeds during germination. These models were fitted to measurement data of oxygen consumption curves for individual germinating seeds of Savoy cabbage, barley and sugar beet provided by Fytagoras. The first model builds on a logistic growth model for the increasing population of mitochondria in the embryo during growth. The other two take the anatomy and physiological properties of the seed into account. One describes the oxygen uptake during the germination phase only. An extension of this model is capable of fitting the complete oxygen consumption curve, including the initial 'repair' phase in which the embryonic cells recover from their dormant state before extensive cell division and growth commences.

Keywords: Modelling, seed germination, cellular respiration, oxygen transport

1 Introduction

At the 90th Study Group Mathematics with Industry (SWI) held at Leiden University from 28 January to 1 February 2013 one of the questions was formulated by the company Fytagoras. Fytagoras is a company that is oriented on science with much expertise in the fields of sensor technology, seed technology and plant breeding. The question concerned the uptake and consumption of oxygen by germinating seeds. Our study considers the seeds of three particular species among the $\sim 250,000$ species of

*Corresponding author

flowering plants: barley (*Hordeum vulgare* L.), sugar beet (*Beta vulgaris*) and Savoy cabbage (*Brassica olerecea* var. *sabauda* L.).

Describing the dynamics of chemical compounds dissolved in liquid solvents (e.g. water) one typically uses the concept of concentration to describe the state of the system. Dealing with mixtures of gasses it is better to use the concept of *partial pressure*. It is the hypothetical pressure of a particular constituent of the gas mixture if the amount of it that is present would have occupied the total volume of the mixture alone, at the same temperature.[1] Gasses dissolve, diffuse and react according to their partial pressures, not their concentrations.

1.1 Some biology of germinating seeds

Seeds consists of at least the following three parts: (1) the *embryo*, which will grow out to become the new plant, (2) a supply of *nutrients* that the embryo can use in the early stage of germination, before it can use light and photosynthesis as main source of energy, and (3) the *seed coat* (or *testa*) that helps to protect the embryo from biotic and abiotic injury and drying out (see Figure 1). The embryo consists of one or two *seed leaves* ('*cotyledons*'), the *hypocotyl* that consists of an embryonic stem and the embryonic root, called the *radical*, and an embryonic shoot (epicotyl) above the point where the cotelydons attach.

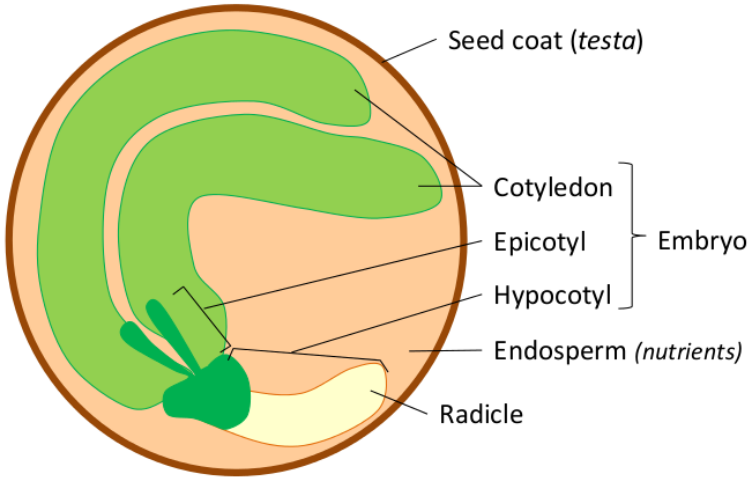

Figure 1: *Seed anatomy of a dicotyledon.*

The detailed internal structure of seeds varies highly among plant species. In some mature seeds the initial food storage tissue that results after fertilisation, the *endosperm*, is still present and contains the nutrients (mainly starch, but may also

[1] Recall the Gas Law: $pV/T = nR$, where $R = 8.314\text{J/mol K}$ is the universal gas constant.

contain oils and proteins) and forms with the seed coat an additional layer around the embryo. These type of seeds are called *endospermic*. Examples are barley and *Arabidopsis thaliana* (see Figure 3). In other, *non-endospermic* seeds, the cotelydons have absorbed all food in the endosperm during seed maturation. The endosperm is almost completely degraded in the mature seeds of this type and the cotelydons serve as sole food storage organ for the embryo. Examples of these are peas, sugar beet and Savoy cabbage.

The cells in a dormant seed are in a dehydrated state: most water content has been removed. Before germination can start the seed needs to get and take up water ('*imbibition*'). Its constituent cells will then take up water, restore and repair their internal biochemical structures and proceed to support the germination process. Typical vegetative cells consist of about 70% water, while dehydrated cells hardly contain any water. We shall call this the *repair phase* of germination. It is shown schematically in Figure 2.

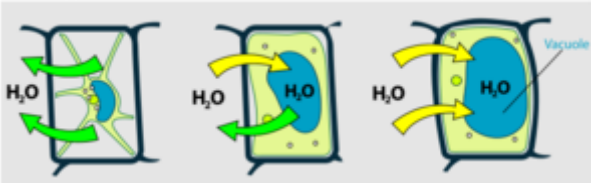

Figure 2: *Water uptake and cell repair.*

After imbibition the seed needs oxygen to germinate, both for repair and the subsequent growth phase in which the radical will start to grow first. The early stage of germination ends when the radical reaches the seed coat and breaks through: a germination event that is known as *testa rupture*. Whether and how much oxygen is available to the embryo for repair and growth depends on several factors, most importantly: *(i)* on the oxygen partial pressure outside the seed, *(ii)* on the consumption of oxygen of the cells inside the seed. i.e. the *respiration rate*, and *(iii)* on the oxygen transport through the seed coat and internal structures towards the embryo. Living seeds start respiration at the moment they start taking up water.

During the repair phase a bit of oxygen is being transported inside with the water. This oxygen is used to produce energy to facilitate the repair process. The repair is necessary because only cells with normal water content can divide and grow. After the repair process is finished and the seeds are fully saturated, the growth begins and the oxygen consumption increases.

The oxygen that the seed takes up has to be transported to the embryo in the middle of the seed because the embryo is the growing part of the seed, and growth can only take place when oxygen is available.

In the transport of oxygen from the seed coat to the embryo several aspects have to be considered that influence the permeability of the oxygen into the seeds. The specific structure of the coat affects the speed of oxygen transport into the seed. After

Figure 3: *Embryo of Arabidopsis thaliana.(M. Bayer; Max Planck Inst. for Developmental Biology)*

the oxygen has passed the seed coat it encounters a layer of starch or oil containing cells, depending on the type of seed. Cabbage, for example, is an oil seed. These cells block direct oxygen transport towards the embryo. It may be absorbed into these cells or pass through the channels in-between. See Figure 4 where a magnification of the layer of starch cells of two different seeds is given. The organisation of these cells varies per type of seed hence the permeability of oxygen differs per type. Moreover, if the space between the cells is very large and the cells lie in an orderly manner, it is much easier for molecules to pass than when the cells are very close together. In Figure 4 the difference in structure between poppy seed and gooseberry seed can be seen.

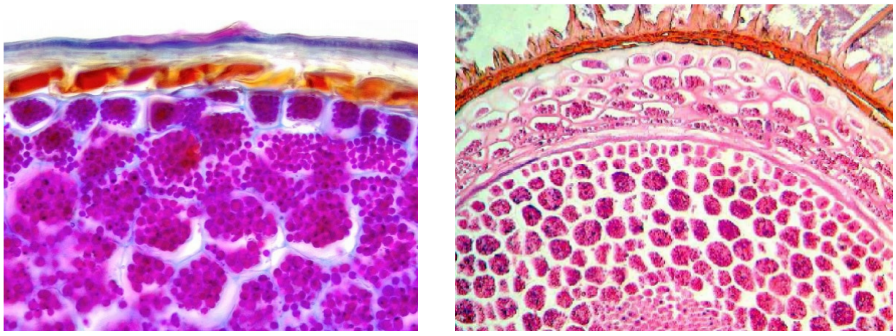

Figure 4: *Close-up images of the seed coat with the starch cells of poppy seed (left) and gooseberry seed (right). The different cell structures can be seen very clearly.*

After the oxygen has made its way through the layer of starch cells, it reaches the embryo. Inside the embryo cells the oxygen enters the mitochondria, which are membrane-enclosed organelles located in the cytoplasm of the cell. These mitochondria are sometimes described as 'cellular power plants' because their main task is to

produce energy that is needed for other processes inside the cell. They produce this energy in the form of ATP molecules by breaking down glucose to carbon dioxide using oxygen. This energy is used for growth, repair and transport in the cell. Note that the number of mitochondria per cell can vary from a few up to hundreds.

We are interested in the connection between oxygen availability and the growth of the embryo, so we will now take a closer look at this growth process. The embryo consists of two parts: an 'idle' part where hardly any growth occurs and the embryonic root (the *radicle*) that grows first to break the seed coat.

Growth of the root occurs by two processes: (1) *cell division* within the growing tip or *apical meristems* that consists of undifferentiated cells that are typically small, having a thin primary cell wall only and which are closely packed together. Their primary function is to divide. For each cell that divides in the meristem, one cell will leave the meristem. However, it need not be that one cell of a pair of daughter cells must become non-proliferative immediately (cf. [9], p.337). Cells that leave the proximal meristem (see Figure 5A) will differentiate into epidermal cells, cortex or stele and (2) *stretch*. Stretching effectively pushes the growth tip downwards. The newly formed cells from the distal meristem differentiate into root cap cells, that protect the apical meristems from rocks, dirt and pathogens. Between the proximal and distal meristems lies the so-called *quiescent center*. It has a much slower cell divison rate than the proximal and distal meristems. Its primary function seems to renew the cells in these meristems [9]. After division, the divided meristematic cell recover to their original size and start building up energy and resources until they have enough to divide again.

An illustration of this process is given in figure 5B. There, it can be seen that the growth tip is being pushed down as the embryo grows. During this process, the size of the growth tip doesn't change, only the idle part enlarges. This process keeps repeating itself until the root tip breaks through the seed coat and the seed has germinated.

1.2 The Q2 machine for non-intrusive oxygen measurements

Single seed oxygen consumption measurements can be made by the so-called '*Q2 machine*' for which Fytagoras developed the underlying measurement technology. It satisfies the criteria that the method is non-invasive, sensitive, fast and cost-effective. We now briefly describe this technique, see Figure 6.

Individual seeds are placed in cylindrical containers in a standard transparent plastic wells plate. A plate with 96 containers is shown in Figure 6. A single container is 10 mm high with a diameter of 5.0 mm, containing on one wall, on the inside, an oxygen sensitive fluorescent coating. When closed by the lid, these containers are almost air-tight. Not completely, because the small oxygen molecules are able to leak slowly through the plastic by diffusion. A 'completely' air-tight container would be too costly. When a light pulse in the blue range of the spectrum is shined on it, the coating will fluoresce a light pulse in the red range with a fluorescence life-time that is indicative of the oxygen level in the container. Outside the container a detector

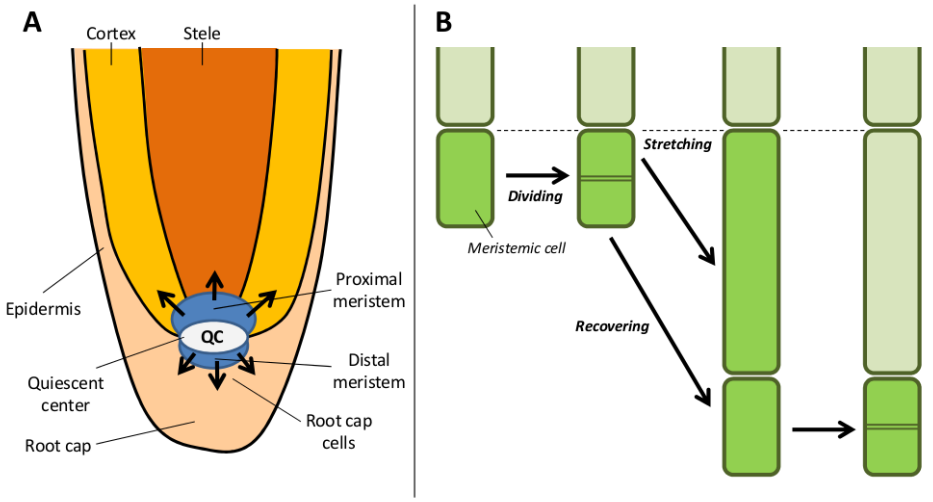

Figure 5: *Schematic presentation of the root apical meristems (growth tips) and differentiated tissues that result (Panel A - following [9]). Stretching of cells, the differentiated cells in particular, pushes down the growth tip (Panel B).*

is placed which measures the intensity and fluorescence life-time of the outgoing red light pulses. In this way one is able to measure regularly and automatically the level of oxygen within the container at high precision without opening it. The seeds are placed on top of filter paper soaked in water or agar to start imbibition.

Figure 7 shows three typical oxygen level curves for a single seed as a function of time. The oxygen level at each time is represented relative to the amount present in the container at the start of the experiment. Temperature is kept constant at room temperature (298 K) during an experiment. The volume in the container exterior to the seed may be assumed constant. That is, the volume of the seed will not expand substantially during early germination. Hence, the oxygen level curve can be interpreted as either change in partial pressure, concentration or total amount of oxygen in the exterior of the seed.

Computing from a container volume of $V_c = 1.9 \times 10^2$ mm^3 (see Table 1), an atmospheric pressure of 1 bar = 100 kPa at sea level and an oxygen content of 21% (by volume), one obtains an initial oxygen content of the container just after closing of

$$n^0_{O_2} = 0.21 \cdot \frac{pV_c}{TR} = 0.21 \times 7.7 \times 10^{-6} \text{ mol} = 1.6 \times 10^{-6} \text{ mol}.$$

Here $R = 8.315$ J/mol$\cdot$K is the gas constant. With a molar mass of 32.00 g/mol, this amounts to 52 μg of O_2 in an empty container. If a seed of e.g. cabbage is placed in the container this reduces slighly, to approximately 51 μg.

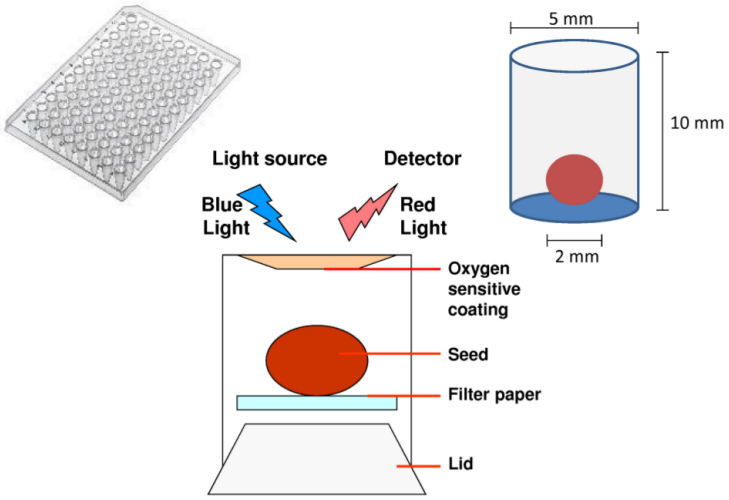

Figure 6: *A schematic presentation of the experimental set-up. A single container in the* 8×12 *well plate has a volume of approximately* 1.9×10^2 mm^3.

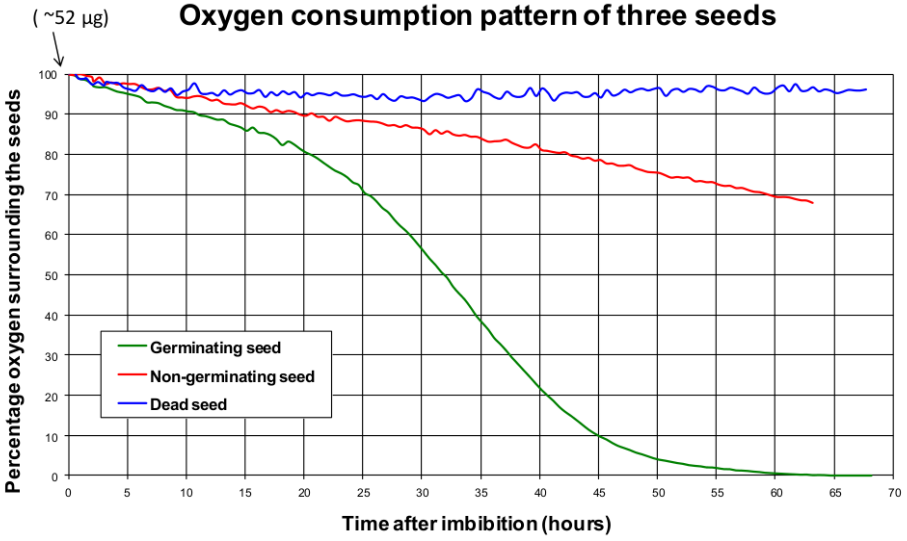

Figure 7: *Three typical oxygen consumption curves as measured by the Q2 machine. Oxygen level surrounding a seed in the container is expressed as fraction of the initial level at the start of the experiment.*

1.3 Problem description

Measured single seed oxygen consumption curves can be used to evaluate the quality of the seed since oxygen consumption is believed to be one of the main characteristics describing quality. However, the interpretation of the data in terms of physical, morphological and physiological properties and processes within the seed is still difficult, due to the lack of knowledge of the basic aspects of gas exchange in seeds and its role in the germination process.

> *The main goal of this study is to interpret characteristics of individual seed oxygen consumption curves as presented in Figure 7 in terms of underlying processes and seed properties.*

We focus on the first stage of germination until the point when the radical breaks through the seed coat, because this is the stage of seed germination in which the data curves are obtained.

1.4 Outline

During the study group we developed three mathematical models for the oxygen consumption of seeds that takes into account current biological knowledge of these processes. The measured oxygen consumption curves as provided by Fytagoras for barley (*Hordeum vulgare* L.), Savoy cabbage (*Brassica oleracea* var. *sabuada* L.) and sugar beet (*Beta vulgaris*) have been fitted to the corresponding curves predicted by these models.

In Section 2 we present a high-level phenomenological model that is able to describe the measured curves for Savoy cabbage and barley well. It results in a correlation among model parameters that can be interesting to look at in more detail (see Section 2.4). In Section 3 we develop a model starting from anatomical considerations in order to investigate the possibilities of relating characteristics of the oxygen consumption curve to seed structure and particular seed properties. In Section 3.4 the latter model is extended.

2 A logistic model for oxygen consumption

The experimental curves of oxygen consumption by germinating seeds of all three different plant species (barley, sugar beet and Savoy cabbage) provided by Fytagoras have a very characteristic 'sigma' shape, similar to the example shown in Figure 7. This indicates that this aspect of the curves originates from a universal underlying mechanism independent of the detailed seed morphology. In this section we propose a mathematical model for respiration of germinating seeds that does not require details on seed anatomy as input, but can reproduce the mentioned characteristic shape of the oxygen consumption curves.

Our central assumption is, that most of the oxygen that is taken up by the seed is consumed by the mitochondria within the cells that constitute the seed. According to the endosymbiotic theory, key organelles in eukaryotic cells, e.g. mitochondria, have evolved from bacteria and still largely behave as such. Bacterial replication under conditions of limited food/oxygen supply is well understood and is governed by the logistic equation.

We set up a general logistic equation for our problem, obtain its analytical solution, and fit it to the provided experimental data by tuning three independent parameters. It turns out that for the majority of the seeds that have been investigated in this study, two of these parameters, namely, the rate of growth of the mitochondria population and the final relative increase in this population, are proportional to each other. We propose a modification of the logistic equation that takes this effect into account.

2.1 Main assumptions

Let us summarize our major assumptions:

Assumption 1. Oxygen consumption happens mainly in mitochondria.

Assumption 2. Although groups of mitochondria are encapsulated inside cells with different biological function, morphology and growth rates, taken all together mitochondria behave as a colony of bacteria, i.e. 'multiplying' at a rate proportional to their number. As with usual bacterial colonies, the population is limited by the available resources, oxygen in particular.

Assumption 3. The rate of oxygen consumption by the seed is proportional to the rate of growth of biomass. In turn, the latter is proportional to the rate of change in the total number of mitochondria in all cells within the seed. There is a maximal number of mitochondria that the seed is able to produce within the closed container.

Assumption 4. The rate of diffusion of oxygen through the cell walls is much faster than the rate of oxygen consumption. Hence, we neglect the (constant) difference between the internal and external concentrations of oxygen.

2.2 Model derivation

We use the following notation:

- O_0 – the initial level of oxygen in a container
- O_c – the critical level of oxygen below which no growth can occur
- m_0 – the initial number of mitochondria
- m_c – the maximum sustainable number of mitochondria

If mitochondria behave as a colony of bacteria, then their number will be changing at the following rate:

$$\frac{dm}{dt} = \alpha m \left(1 - \frac{m}{m_\mathrm{c}}\right), \tag{1}$$

where α is the maximum rate of growth. This is a *logistic equation* with the well-known analytical solution

$$m(t) = \frac{m_\mathrm{c}}{1 + \left(\frac{m_\mathrm{c}}{m_0} - 1\right) e^{-\alpha t}}, \tag{2}$$

which satisfies the initial condition $m(0) = m_0$. *Assumption 3* can be written as

$$\frac{dO}{dt} = -\beta \frac{dm}{dt}. \tag{3}$$

It leads to the following equation for the amount of oxygen present in a container at time t:

$$O(t) = C - \beta m(t), \tag{4}$$

where the constants β and C must be such that

$$O(0) = O_0, \quad \lim_{t\to\infty} O(t) = O_\mathrm{c}. \tag{5}$$

Solving these equations for β and C gives:

$$C = O_0 + m_0 \frac{O_0 - O_\mathrm{c}}{m_\mathrm{c} - m_0}, \quad \beta = \frac{O_0 - O_\mathrm{c}}{m_\mathrm{c} - m_0}. \tag{6}$$

The final equation for the amount of oxygen is thus

$$O(t) = O_0 + \frac{O_0 - O_\mathrm{c}}{m_\mathrm{c} - m_0} \left[m_0 - \frac{m_\mathrm{c}}{1 + \left(\frac{m_\mathrm{c}}{m_0} - 1\right) e^{-\alpha t}} \right]. \tag{7}$$

Introducing the normalized quantities,

$$\tilde{O}(t) = \frac{O(t)}{O_0}, \quad \tilde{O}_\mathrm{c} = \frac{O_\mathrm{c}}{O_0}, \quad \tilde{m}_\mathrm{c} = \frac{m_\mathrm{c}}{m_0} \tag{8}$$

we arrive at the dimensionless result:

$$\tilde{O}(t) = 1 + \frac{1 - \tilde{O}_\mathrm{c}}{\tilde{m}_\mathrm{c} - 1} \left[1 - \frac{\tilde{m}_\mathrm{c}}{1 + (\tilde{m}_\mathrm{c} - 1)\, e^{-\alpha t}} \right]. \tag{9}$$

Note that the measured oxygen consumption curve as presented e.g. in Figure 7 shows $\tilde{O}(t)$. The functional expression (9) for the latter has three parameters that allow it to be fitted to the experimental data.

2.3 Fitting results

Figure 8 shows the normalized measured oxygen levels for 91 barley seeds and the corresponding curves obtained by fitting with expression (9). To determine these parameters we have used a standard nonlinear least squares optimization routine with the lower bounds set as: $\tilde{m}_c \geq 1$, $\tilde{O}_c \geq 0$, and $\alpha \geq 0$. Figure 9 shows the

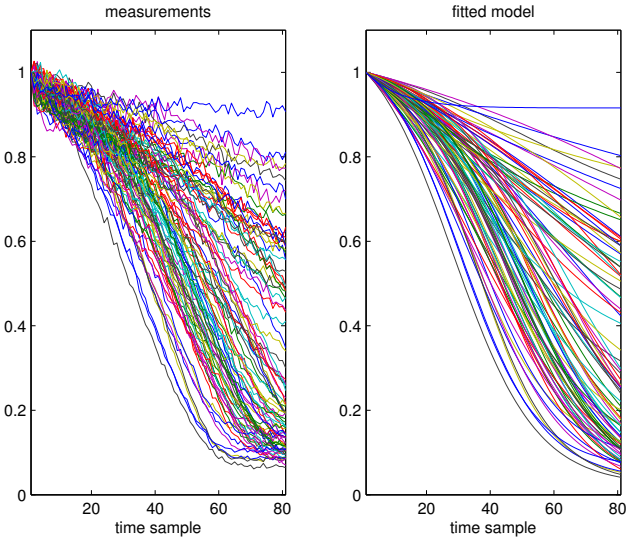

Figure 8: *Left: Measured oxygen consumption for 91 individual barley seeds at* 295 K *over a time period of 80 hours. Right: fitted logistic model.*

experimental curves and the corresponding fits for 24 Savoy cabbage seeds.

2.4 Conclusions and discussion

A closer look at the mutual relation between the three fitted parameters in different experiments reveals an interesting tendency. Namely, the growth rate parameter α appears to depend almost linearly on the relative total population increase $\tilde{m}_c = m_c/m_0$, so that when α is plotted against $1/\tilde{m}_c$ one gets a pronounced hyperbolic curve – see Figure 10. In other words the ratio $\alpha/\tilde{m}_c = k$ is close to a constant. This behavior indicates that instead of (1) the following form of the logistic equation should be used from the start:

$$\frac{dm}{dt} = km\left(\frac{m_c}{m_0} - \frac{m}{m_0}\right), \tag{10}$$

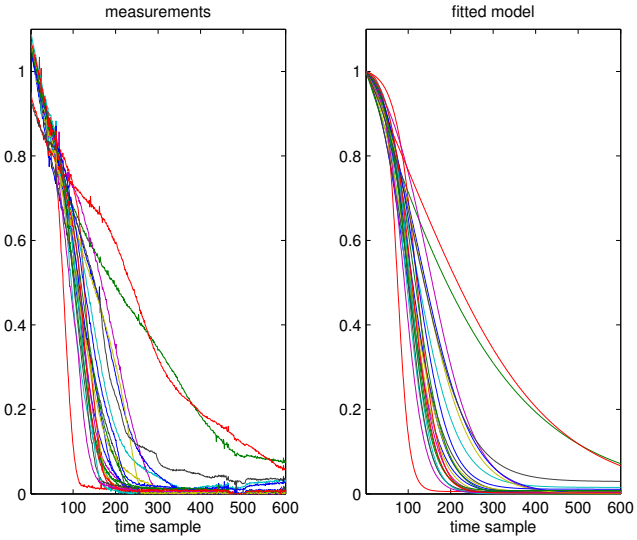

Figure 9: *Left: Measured oxygen consumption for* 24 *individual Savoy cabbage seeds at* 293 K. *Time samples were taken each 30 min. Right: fitted logistic model.*

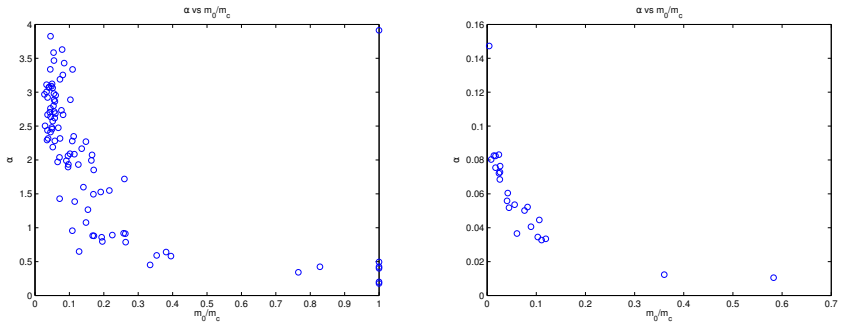

Figure 10: *Apparent hyperbolic dependence of the growth parameter* α *on the inverse of the relative total population growth* $1/\tilde{m}_c$, *i.e.,* $\alpha \approx km_c$ *for some constant* $k > 0$. *Left – barley , right – Savoy cabbage.*

so that the original standard logistic equation (1) is recovered under the assumption

$$\alpha = k\tilde{m}_c. \tag{11}$$

Of course, the actual values of all fitted parameters reconstructed in our simulations should not be taken too literally as we have used a normalized time axis. This fact, however, does not invalidate our conclusions about the mutual relation between the fitted parameters. In any case, further interpretation of the biological meaning of these parameters will require a much wider statistical analysis in an absolute time frame (say, in hours), as well as deeper understanding and an additional mathematical model of the apparent link between the growth rate and the final relative increase in the mitochondria population.

3 An anatomically structured model for oxygen uptake

As mentioned in Section 1.3, the main objective is to interpret the characteristics of the oxygen consumption curve in terms of physical, biological and morphological properties of the seed. The logistic model that we discussed in the previous section cannot be used for such explanatory purposes as it does not take any details of underlying shape or processes into account in its derivation.

In this section we take a first step in developing a mathematical model for oxygen uptake in a germinating seed that can be used to assess seed quality using oxygen consumption measurements. We have chosen to focus on a seed with the simplest morphology: the Savoy cabbage seed (*Brassica oleracea* var. *sabuada* L.). These have an almost perfect spherical appearance, with a radius of approximately 1.5 mm. Although its external shape is simple, internally the anatomy can still be quite complicated. Sugar beet seeds (*Beta vulgaris*) for example have a much more complicated morphology both externally and internally.

3.1 Driving processes and their time and spatial scales

We identify four processes that play a major role in the early germination stage of the seed.

P0. The process of water uptake (*imbibition*), that allows the embryonic cells to restore their water content, repair the internal molecular constitution and start functioning 'normally' in the early germination stage, i.e. targeted at supporting growth of the embryonic root (the *radical*).

P1. The process of *oxygen diffusion*: first through the seed coat and next through the seed's interior to reach the embryonic cells where it is finally used in metabolism.

P2. The process of *celullar respiration*, i.e. the oxygen uptake and consumption by the cells in the seed.

P3. The process of *asymmetric cell division* of the embryonic cells in the growth tip in the radical that results in growth. (We shall discuss this process in more detail below).

The initial repair process P0 is hard to describe in detail. In view of the oxygen consumption curve it corresponds to the first 15 hour time period in Figure 7, when oxygen consumption appears to happen at an approximately constant rate. We shall ignore this phase and focus on capturing the increased consumption rate and later steady decrease. Hence, we assume that P0 has been completed and only consider P1, P2 and P3.

As a first step toward the deduction of the model it is important to assess the characteristic time scales of processes P1–P3 (see e.g. [6]). We will use the available experimental data as much as possible. Otherwise, assumptions will be made. Awareness of these time scales motivates modelling decisions concerning its mathematical structure: i.e. whether the model will be formulated in terms of either ordinary differential equations or partial differential equations, depending on whether the processes involving the spatial variables can be neglected.

We now consider processes P1–P3 in further detail.

3.1.1 Oxygen uptake through seed coat and internal diffusion

The seed coat forms a barrier for oxygen transport. The physical and biochemical details of oxygen uptake through the seed coat, which is part of P1, are largely unknown. The application of artificial coatings to the seed coat are known to strongly influence oxygen uptake. Therefore, this process is taken as an important unknown in our model. Measurements have been performed on the permeability of the skin of fruits like apple, pear and nectarine though, cf. [8]. Such results for the seed coats of seeds of cabbage or sugar beet were not found in the literature.

The seeds of all species discussed in the report will have a complicated internal structure (cf. Figure 4). It is possible that there is free intercellular space in cell tissue through which oxygen and carbon dioxide can diffuse freely (see e.g. the free intercellular space volumes reported for flesh tissue in fruits like apple, pear and nectarine ranging from 17 to 2% respectively, cf. [8]). Similar structures are expected in seeds, but quantitive information was lacking. However, imbibition may have caused such channels to become water-filled. This makes a great difference for the effective diffusivity of oxygen through the cell tissue from the seed coat to the tissue where it is consumed most during germination. In fact, diffusion of oxygen in air is four orders of magnitude faster than that in water (cf. [2, 7]). The estimated diffusivity of oxygen in fruit flesh tissue is approximately 1.5×10^{-7} m^2/s on average [8].

Diffusivity:	Value:	Description:
$D_{\mathrm{O_2-water}}$	2×10^{-9} m^2/s	Diffusivity of oxygen in water at 298 K (Wilke & Chang [2])
$D_{\mathrm{O_2-air}}$	1.8×10^{-5} m^2/s	Diffusivity of oxygen in air at standard temperature (273 K) and pressure (1013 hPa; Massman [7], Table 8).
$D_{\mathrm{O_2-fruit}}$	$0.3 - 2.7 \times 10^{-7}$m^2/s	Estimated diffusivity of oxygen in fruit flesh (at 293 K, Rajapakse *et al.* [8]).

Collis-George & Melville [3] computed and discussed oxygen distribution profiles in four models for a spherical seed with specific assumptions on the properties of cellular respiration. In these models it is assumed that all seed tissue cells respire in the same fashion, i.e. the functional description for the local oxygen consumption rate is the same throughout the whole seed. In our study, we assume that most of oxygen uptake takes place in the dividing embryonic root cells. A steep oxygen gradient as predicted by the models in [3] in the tissue between seed coat and embryonic root is then expected to be more shallow. No measurements were available to support the theoretically reasonable oxygen gradient from seed coat to embryonic root by experimental data.

The time scale of convergence to a homogeneous steady state has been investigated numerically in a one-dimensional linear diffusion problem

$$\frac{\partial u}{\partial t} = D\frac{\partial^2 u}{\partial x^2} \qquad \text{on } [0, 1.7]$$

(in units mm and s for length and time). We took $D = 2 \times 10^{-3}$ mm^2/s, the minimal reported diffusivity for oxygen. In other cases equilibration will be faster. The initial condition is a step-wise normalized oxygen distribution u_0:

$$u_0(x) = \begin{cases} 0, & x \in [0, 1.5], \\ 1, & x \in (1.5, 1.7]. \end{cases}$$

Neumann boundary conditions (i.e. zero-flux) are imposed at both boundaries.

The computed evolution of the normalized oxygen concentration profile is shown in Figure 11. The system equilibrates on a time scale

$$T_d \approx 700 \text{ s} \approx 12 \text{ min} = 0.2 \text{ h}.$$

The partitioning of oxygen between water and air is given by Henry's Law,

$$[\mathrm{O_2}]_{\mathrm{water}} = k_{H,cp}\, p_{\mathrm{O_2}}, \tag{12}$$

where the Henry's Law constant $k_{H,cp}$, or oxygen solubility, equals 12 μM/kPa [5, 4] (at 293 K). Equivalently one may use the dimensionless Henry's Law constant k_H in terms of concentrations:

$$[\mathrm{O_2}]_{\mathrm{water}} = k_H\, [\mathrm{O_2}]_{\mathrm{air}},$$

where $k_H = 0.03$ at 293 K.

3.1.2 Cellular respiration: oxygen uptake and consumption

Detailed information on cellular respiration of (different types of) cells in seeds is hard to obtain. Rajapakse *et al.* [8] provide measured respiration rates for some fruits. Detailed measurement of changes in cellular respiration as a function of external oxygen pressure around mammalian cells (e.g. rat cardiomyocytes and human umbilical

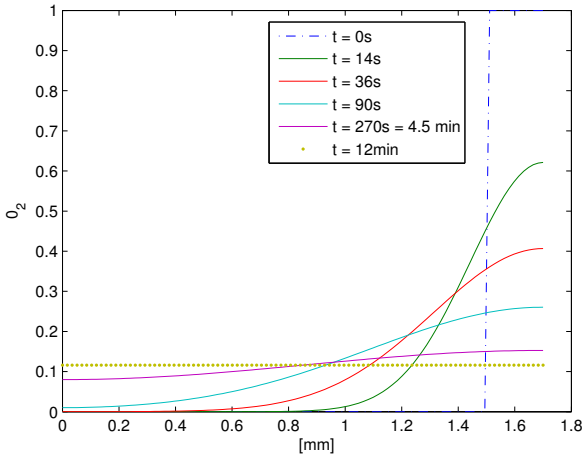

Figure 11: *Convergence to homogeneous steady state for oxygen diffusing in water at 298 K. Oxygen concentration has been normalized.* $D = 2 \times 10^{-3}$ mm^2/s.

vein endothelial cells) and isolated mitochondria from different types of rat cells have been reported in [5]. The drop in oxygen partial pressure within cells (myocytes) and a stagnant layer around cells is considered in [4].

Being aware that one cannot simply apply results for animal cells to the setting of plant cells, we nevertheless use the results on [5] as an indication of the order of magnitude of cellular respiration rates and a reasonable mathematical form for the functional dependence of this rate on partial oxygen pressure p_{O_2}. In fact, [5] finds that the oxygen flux J into uncoupled human umbilical vein endothelial cells in cell suspension can be fitted well by a hyperbolic curve

$$J = \frac{J_{\max}\, p_{O_2}}{p_{50} + p_{O_2}}, \tag{13}$$

with maximal flux per cell of $J_{\max} = 0.035$ fmol/s and an environmental oxygen pressure of $p_{50} = 0.023$ kPa at which the oxygen flux is at halve-maximal level (cf. [5], Figure 3, p.591; temperature is 37°C; single cell oxygen flux has been computed from the data provided in *loc.cit.* for a cell population). Coupled endothelial cells show a slightly increased maximal flux and 3-fold larger p_{50} (namely 0.068 kPa). An increase of the latter is expected: oxygen levels in the middle of a cluster will be lower than in cells at the outer end. Thus, a higher oxygen partial pressure is needed outside the cluster to reach the same (average) overall respiration rate.

3.1.3 Time scale of cell division and root growth

A central question in plant physiology is to determine the processes that regulate their growth. Growth rate is regulated by the combined activity of cell production by cell division and expansion of the cells that are already present [1]. Modelling root growth in detail is a complex project in itself, see [1, 9] and the references found there. The duration of the time between two consecutive cell divisions of the same meristematic cell (the *cell cycle*, recall Section 1.1, Figure 5 in particular) has been measured and is of the order of 10–15 hours [9].

We consider a very rudimentary model only. That is, the rate at which the root length r increases will be assumed proportional to the amount of oxygen consumed in the growth tip (i.e the root proximal meristem, recall Section 1.1), with proportionality constant ρ.

From the experimental oxygen consumption curves for Savoy cabbage (see e.g. the ensemble-averaged curve presented in Figure 14) one estimates that the duration T_g of the growth phase, from start to rupture of the seed coat, is approximately 60 hours. We assume that the radicle needs to extend over a length L equal to the diameter of the seed to do so. That is, in the setting of cabbage seeds, $L = 3$ mm.

A meristematic cell has length ℓ of approximately 15 μm and will stretch after differentiation with a factor σ_f to reach its final length. The length of the differentiated cell is a function of its distance to the quiescent center (cf. [1], Fig. 3). We ignore this effect and take an average value $\sigma_f = 4$ instead. Thus, in a time T_g, at least

$$N = \frac{L}{\sigma_f \ell} = 50$$

differentiated cells in a row must have been formed from the proximal meristem to realise an extension of the radicle over length L. Consequently, each

$$\Delta t = \frac{T_g}{N} = 1.2 \text{ h}$$

a new differentiated cell must appear in a linear array of differentiated cells in the growing root.

3.2 Model formulation

The closed container in which the seed is placed is represented by a perfect cylindrical domain of height h and radius R_c. The seed is modelled as a sphere of radius R_s, which is reasonable for seeds of Savoy cabbage (*Brassica oleracea* var. *sabuada* L.) of which we used the data provide by Fytagoras. The radical (embryonic root) inside the seed is cylindrically shaped too, with radius R_r. The cross sectional area of the radical, A, therefore equals πR_r^2. The radical is divided into a growth tip, of volume V_{tip} and the elongated, differentiated root cells, see Figure 3.2.

The oxygen partial pressure within the closed container, outside the seed, O_e, is considered homogeneously distributed. The oxygen partial pressure inside the seed is

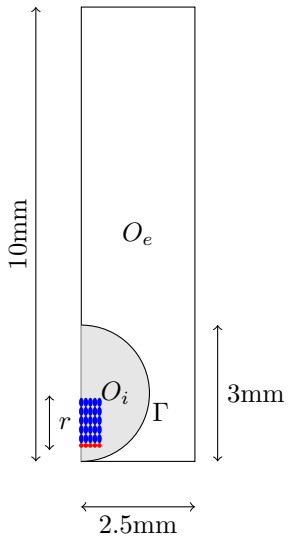

Figure 12: *The model geometry is axisymmetrical. Red cells: growth tip; blue cells: elongated and differentiated root cells that appeared by cell division after start of experiment (remainder of embryo is not shown).*

represented by O_i. As a first modelling approach and motived by the fast equilibration of the oxygen distribution in water on the time scale of cell division (see Section 3.1.1), we take O_i homogeneously distributed within the seed for simplicity, because of lack of more detailed information on oxygen gradients inside the seed.

Due to growth the radical will elongate. The elongation length of the radical at time t is $r(t)$. We ignore any bending in the radical when computing the additional root volume due to radical growth. No experimental observations were available for both elongation and shape of the radical during the early germination phase that could support more elaborate hypotheses. Thus, in the proposed model, the seed coat is the main oxygen barrier that separates the embryo from the free exterior oxygen in the container.

Variable:	Variable name:
External oxygen partial pressure	$O_e = O_e(t)$
Internal oxygen partial pressure	$O_i = O_i(t)$
Total elongation of radical due to growth	$r = r(t)$

Changes in volume of seed (or container) are ignored. Since experiments are performed under constant temperature, we may consider the oxygen partial pressures in the interior and exterior domains as proportional to concentrations, with constant proportionality everywhere. We shall do so from this point on.

The precise biophysical mechanisms of oxygen uptake through the seed coat at microscopic scale are largely unknown. In our model we take the simplest modelling

approach, by representing the seed coat as a barrier with unknown permeability a for oxygen (of dimension of velocity). The total flux of oxygen from the exterior into the seed through the seed coat is then given by

$$J_{sc} := aS_\Gamma(R^*O_e - O_i), \tag{14}$$

where R^* is the so-called *accumulation ratio* and allows for modelling asymmetric transport properties of the barrier. S_Γ is the total area of the spherical seed coat: $S_\Gamma = 4\pi R_s^2$. At steady state, i.e. when there is no flux through the barrier, $O_i = R^*O_e$. We have taken $R^* = k_H$, Henry's Law constant, thinking of oxygen dissolving into water inside the seed.

The uptake of oxygen by cells in the embryo and any remaining cells in the endosperm is considered to be due mainly to mitochondrial activity, which depends on the oxygen partial pressure (see [5]). We let $J(O_i)$ denote the average amount of oxygen consumed by cells per unit time per unit volume. It is of the form:

$$J(O_i) = \frac{J_{max}O_i}{J_0 + O_i} \tag{15}$$

(see Section 3.1.2). We allow cells in the growth tip to consume a factor α more than this average amount, because these cells are most active.

We thus arrive at the following model equations:

$$V_i\frac{dO_i}{dt} = -J(O_i)(\alpha V_{\text{tip}} + Ar + V_i) + aS_\Gamma(k_HO_e - O_i), \tag{16}$$

$$V_e\frac{dO_e}{dt} = aS_\Gamma(O_i - k_HO_e), \tag{17}$$

$$\frac{dr}{dt} = \rho J(O_i)V_{\text{tip}}, \tag{18}$$

with initial conditions

$$O_i(0) = O_{i,0}, \qquad O_e(0) = O_{e,0}, \qquad r(0) = 0. \tag{19}$$

The factor ρ in equation (18) is the oxygen-to-root biomass conversion factor. It measures the amount of oxygen needed in the growth tip to divide, differentiate and stretch to produce root biomass in terms of increased root length.

3.3 Fit to experimental data

The model equations (16)–(18) contain 12 parameters and two initial conditions. The dimension of this parameter space is too high to determine all of them from the experimental data that gives detailed time series of just one component of the solution only. The approach would be to solve an optimisation problem to minimize the distance between the solution of the model equations and the averaged experimental curve for a suitably chosen objective function. There may be difficulties in solving the

optimisation problem due to this limited information. Moreover, even if a sufficiently good solution is found, some of the parameters obtained may not be in a biologically reasonable range, causing interpretation issues.

However, some of the parameters and initial conditions can be estimated *a priori*, based on the given geometry of the experimental environment, anatomical information on the seeds and values found in the literature (often for other organisms however). In Section 3.3.1 we discuss these estimates that allow us to reduce the number of unknown parameters to two: the seed coat permeability a and the excess oxygen consumption factor α.

3.3.1 *A priori* estimating model parameters

Table 1 summarizes the parameter values that can be fixed by the geometric set-up of the experiments and seed morphology. We now discuss the constraints imposed on physiological parameter values using information found in the literature (see Sections 3.1.1–3.1.3) and the estimation of initial values.

The initial external oxygen concentration outside the seed just after the container has been closed, O_e^0 can be computed using an atmospheric pressure of 100 kPa, temperature of 293 K and oxygen content of 20%:

$$\begin{aligned} O_e^0 &= 0.2 \times \frac{p}{TR} = 0.2 \times \frac{100 \text{ kPa}}{293 \text{ K} \cdot 8.315 \text{ L/mol K kPa}} \\ &= 8.21 \times 10^{-3} \text{ mol/L} = 2.6 \times 10^{-4} \text{ mg/mm}^3. \end{aligned}$$

We assume that the initial internal oxygen concentration at that time is at equilibrium with the external initial oxygen concentration over the seed coat barrier:

$$O_i^0 = k_H O_e^0 = 0.03 \times 2.6 \times 10^{-4} \text{ mg/mm}^3 = 7.8 \times 10^{-6} \text{ mg/mm}^3.$$

The model (16)–(19) describes the oxygen consumption during the growth phase, following the repair phase. The start of the growth phase has been determined by visual inspection of average oxygen consumption curve (i.e. the consumption curve by averaging the individual curves of all seeds in the experimental run). It is taken at approximately time $t = 30$ h after the start of the experiment (see Figure 14). At that time, the oxygen level within the container has dropped to 79% of the initial level. At the end of the experiment, it has dropped to 19% of the initial level. The initial conditions $O_{e,0}$ and $O_{i,0}$ are computed from O_e^0 and O_i^0 by taking this reduction into account:

$$O_{e,0} = 0.79 \times O_e^0, \qquad O_{i,0} = 0.79 \times O_i^0.$$

Gnaiger *et al.* [5] report on various values for the oxygen partial pressure within the cells such that cellular oxygen consumption or mitochondrial oxygen consumption is at halve-maximal value. At 298 K, these values are in a range of roughly 0.005–0.08 kPa for mitochondria in animal cells, with a bias towards the lower values in the

Name:	Value:	Unit:	Description:
Geometric constants:			
R_c	2.5	mm	Radius of the cylindrical container
h	10	mm	Height of of the cylindrical container
R_s	1.5	mm	Radius of the spherical seed
R_r	0.5	mm	Radius of radical (root)
ℓ	1.5×10^{-2}	mm	Length of cells in growth tip
σ_f	4	–	Stretch factor
Computed geometric attributes:			
V_i	14.1	mm^3	Seed volume
V_c	196	mm^3	Volume of container
V_e	182	mm^3	Volume inside container exterior to seed
V_{tip}	0.0236	mm^3	volume of growth tip
S_Γ	28.3	mm^2	Seed coat area
A	0.79	mm^2	Cross sectional area of radical
Physical parameters:			
k_H	0.03	–	Henry's constant for oxygen in water
Estimated initial conditions (see Section 3.3.1):			
O_e^0	2.6×10^{-4}	$\mathrm{mg\,mm^{-3}}$	O_2 concentration outside seed at closure container
O_i^0	7.8×10^{-6}	$\mathrm{mg\,mm^{-3}}$	O_2 concentration inside seed at closure container
$O_{e,0}$	2.1×10^{-4}	$\mathrm{mg\,mm^{-3}}$	Initial oxygen concentration outside seed
$O_{i,0}$	6.2×10^{-6}	$\mathrm{mg\,mm^{-3}}$	Initial oxygen concentration inside seed
Estimated physiological parameters (see Section 3.3.1):			
J_{max}	3.6×10^{-3}	$\mathrm{mg\,mm^{-3}\,h^{-1}}$	Maximal oxygen consumption per tissue volume
J_0	3.2×10^{-7}	$\mathrm{mg\,mm^{-3}}$	O_2 level at $\frac{1}{2}J_{max}$ O_2-consumption
ρ	5.9×10^3	$\mathrm{mm\,mg^{-1}}$	Oxygen-to-root biomass conversion factor
L	3	mm	Elongation of the radical at time of testa rupture
Results of fitting: (see Section 3.3.2):			
a	7	$\mathrm{mm\,h^{-1}}$	Seed coat permeability for oxygen
α	2	–	Excess oxygen consumption factor

Table 1: *Parameter settings in the anatomically structured model for the growth phase and results of fit.*

range. We take 0.025 kPa. This yields an intracellular oxygen concentration of

$$\begin{aligned} J_0 &= \frac{p_{O_2}}{RT} = \frac{0.025 \text{ kPa}}{8.315 \text{ kPa L/mol K} \cdot 298 \text{ K}} = 1.0 \times 10^{-5} \text{ M} \\ &= 3.2 \times 10^{-7} \text{ mg/mm}^3. \end{aligned}$$

We ignore at this point the effects of an intracellular oxygen gradient from cell membrane towards the mitochondria.

Moreover, Gnaiger *et al.* [5] provide values for the maximal oxygen consumption of human umbilical vein endothelial cells of $80 - 100$ pmol/s per cm^3 of experimental medium that contained 2.6×10^6 cells per cm^3. For the value of 100 pmol/s this implies a maximal consumtion rate of 0.038 fmol/s per cell. For a cylindrical cell with a length of 15 μm and diameter of 10 μm (i.e. of volume 1.2×10^{-6} mm^3), this amounts to

$$J_{max} = 3.1 \times 10^4 \text{ fmol/mm}^3 \text{ s} = 3.6 \times 10^{-3} \text{ mg/mm}^3 \text{ h}.$$

The oxygen-to-biomass conversion factor ρ can be estimated in the following manner. The oxygen consumption function $J(O_i)$ is such that it has a quite sharp switch between maximal consumption and almost no consumption (cf. [5]). So we assume that it operates at maximal value for most of the growth phase. Therefore,

$$\rho \approx \frac{\Delta r}{\Delta t} \cdot \frac{1}{J_{max} \cdot V_{tip}} = \frac{3 \text{ mm}}{60 \text{ h}} \cdot \frac{1}{8.5 \times 10^{-5} \text{ mg/h}} = 5.7 \times 10^3 \text{ mm/mg}.$$

3.3.2 Fitting results

The remaining two parameters, a and α, in the model were determined by solving an optimisation problem to fit the experimental data. As targets in the optimisation process the following were considered:

- The ensemble-averaged time history $O_e^*(t)$ of the measured external oxygen level;
- The final root length $r_f^* := r(T_g) = L$.

The optimisation problem consisted of minimising the cost function

$$F = \|O_e - O_e^*\|_2^2 + w|r(T_g) - r_f^*|^2,$$

where $w > 0$ is a weight to give more or less importance to unevenness in the final root length. The results for parameters a and α are shown in Table 1. A simulation result of the model for these parameter values is shown in Figure 13.

The value for a, which is 7 mm/h $= 2 \times 10^{-6}$ m/s, seems to have a reasonable order of magnitude, when compared to values for the permeability of cell membranes for plant hormones, like auxin. However, no information on seed coat permeability for oxygen was avaible to compare this value with.

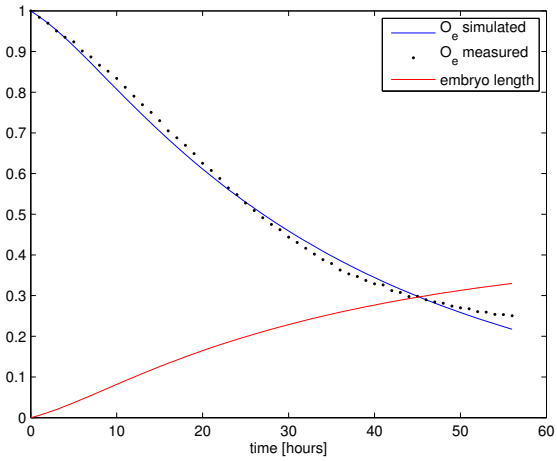

Figure 13: *Simulation result for the anatomically structured model* (16)–(19) *for the growth phase with parameter settings as summarised in Table 1. The data are obtained from Savoy cabbage.*

3.4 An extended model including the initial repair phase

The model (16)–(19) does not describe the repair phase that preceeds the growth phase. In this section we suggest an extension of the former model, which can be used to fit the entire oxygen consumption curve, including the initial repair process. Moreover, the experimental oxygen consumption curve is almost flat after approximately 80 hours. This fact seems difficult to account for directly with the oxygen consumption function $J(O_i)$ that was used in the previous model.

We suggest two modifications. Firstly, we realise that a higher oxygen level outside the growing cells is needed to create an internal oxygen concentration at the mitochondria to keep these 'maximally' functioning (see e.g. [4]). The simplest way to include this into the model, is to introduce a threshold value $\tilde{O}_i$ for the oxygen concentration outside the cells: if the oxygen concentration is below this value, the intra-cellular concentration near the mitochondria becomes so low that they stop functioning. This is realised mathematically by replacing O_i in $J(O_i)$ by $(O_i - \tilde{O}_i)_+$, where $(x)_+$ is the positive part of x:

$$(x)_+ := \begin{cases} x, & \text{if } x \geq 0, \\ 0, & \text{if } x < 0. \end{cases}$$

Secondly, in model (16)–(19) we implicitly assumed that all cells in the embryonic root need the same, fixed, time to complete their repair phase and start the growth phase. A more relaxed assumption is that these times are normally distributed.

Thus, in our extended model, equations (16)–(18) remain the same except for

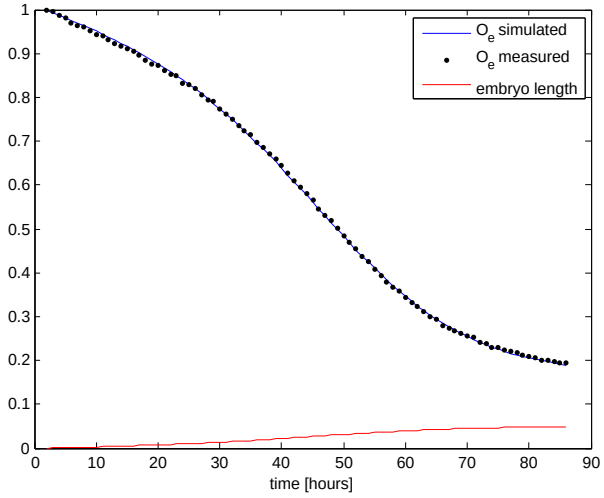

Figure 14: *The computed oxygen consumption curve using the extended model (blue line), compared to the experimental values (black dots). The growth phase starts at approximately* $t = 30$ h*, when the oxygen level has dropped to* 79%*. The length of the growing tip is shown as well. The data are obtained from Savoy cabbage seeds.*

replacing $J(O_i)$ in (16) by the time-dependent function

$$\tilde{J}(O_i, t) := f(t) \frac{J_{max}(O_i - \tilde{O}_i)_+}{J_0 + (O_i - \tilde{O}_i)_+}, \tag{20}$$

where

$$f(t) = 1 + \epsilon + \mathrm{erf}(c_1 t - c_2), \tag{21}$$

with $\mathrm{erf}(x)$ the *error function*:

$$\mathrm{erf}(x) := \frac{2}{\sqrt{\pi}} \int_0^x e^{-\xi^2}\, d\xi.$$

The error function is a strictly increasing function with horizontal assymptotes at -1 and 1 when x tends to $-\infty$ and $+\infty$ respectively. It has a sigmoidal shape, is point symmetric with respect to 0 and takes values in $(-1, 1)$. As initial conditions in the extended model we take

$$O_e(0) = O_e^0, \qquad O_i(0) = O_i^0.$$

The two parameters c_1 and c_2 are related to the standard deviation and the mean of the normally distributed damage, respectively. Here ϵ is a small positive number,

Name:	Value:	Unit:	Description:
Physiological parameters:			
$\tilde{O}_i$	1.3×10^{-6}	$\mathrm{mg\,mm^{-3}}$	O_2 concentration threshold in the seed
J_{max}	2.7×10^{-2}	$\mathrm{mg\,mm^{-3}\,h^{-1}}$	Maximal oxygen consumption per tissue volume
J_0	3×10^{-8}	$\mathrm{mg\,mm^{-3}}$	O_2 level at $\frac{1}{2}J_{max}$ O_2-consumption
Results of fitting:			
a	25	$\mathrm{mm\,h^{-1}}$	Seed coat permeability for oxygen
α	1.8	–	Excess oxygen consumption factor
ϵ	1×10^{-3}	–	
c_1	1.8×10^{-2}	$\mathrm{h^{-1}}$	
c_2	2.37	–	

Table 2: *Parameter settings in the extended anatomically structured model and results of fit. Only new parameters and settings that differ from those mentioned in Table 1 are shown.*

reflecting the fact that there are some mitochondria that function from the very beginning.

The newly introduced parameter $\tilde{O}_i$ can be easily estimated from the right end of the measured oxygen consumption curve in Figure 14. The oxygen level has then dropped to 19% of the initial level, but still has not completely saturated. We therefore take $\tilde{O}_i$ at 17% of the initial level:

$$\tilde{O}_i = 0.17 \times O_i^0 = 1.3 \times 10^{-6}\ \mathrm{mg/mm^3}.$$

We estimated by hand the values of the remaining parameters. Similarly as described in Section 3.3.1. We had to increase J_{max} by a factor 7.6 and we used the refinement $J_0 \approx 3 \times 10^{-8}$ mg/mm^3. A summary of the modified and additional parameter settings together with the fitting results is given in Table 2. The resulting oxygen consumption curve, plotted together with the averaged experimental data is shown in Figure 14.

References

[1] G.T.S. Beemster and T.I. Baskin (1998). Analysis of cell division and elongation underlying the developmental acceleration of root growth in *Arabidopsis thaliana*. *Plant Physiol.* **116**: 1515–1526.

[2] C.R. Wilke and P. Chang (1955). Correlation of diffusion coefficients in dilute solutions. *AIChE Journal* **1**(2): 264–270. DOI: 10.1002/aic.690010222.

[3] N. Collis-George and M.D. Melville (1974). Models of oxygen diffusion in respiring seed, *J. Exp. Botany* **25**(89): 1053–1069.

[4] K.E. Dionne (1990). Oxygen transport to respiring myocytes, *J. Biol. Chem.* **265**: 15400–15402.

[5] E. Gnaiger, R. Steinlechner-Maran, G. Méndez, Th. Eberl and R. Margreiter (1995). Control of mitochondrial and cellular respiration by oxygen, *J. Bioenergetics and Biomembranes* **27**(6): 583–596.

[6] J. Mauseth (2011). *An Introduction to Plant Biology*, Jones & Bartlett Learning.

[7] W.J. Massman (1998). A review of molecular diffusivities of H_2O, CO_2, CH_4, CO, O_3, SO_3, NH_3, N_2O, NO, and NO_2 in air, O_2 and N_2 near STP, *Atmospheric Environment* **32**(6): 1111–1127.

[8] N.C. Rajapakse, N.H. Banks, E.W. Hewett and D.J. Cleland (1990). Development of oxygen concentration gradients in flesh tissues of bulky plant organs, *J. Amer. Soc. Hort. Sci.* **115**(5): 793–797.

[9] P.L. Webster and R.D. MacLeod (1980). Characteristics of root apical meristem cell population kinetics: a review of analyses and concepts, *Environmental Exp. Bot.* **20**: 335–358.